

Optical Tomography by Digital Holographic Microscopy

Nicolas Pavillon*, Jonas Kühn, Florian Charrière, Christian Depeursinge

Advanced Photonics Laboratory, Ecole Polytechnique Fédérale de Lausanne (EPFL), CH-1015 Lausanne, Switzerland

*Corresponding author: nicolas.pavillon@a3.epfl.ch

Abstract: Three-dimensional imaging coupled with quantitative phase signal gives rise to 3D refractive index reconstruction, leading to interesting perspectives for cell observation. We present results of tomographic measurements, taken in the framework of digital holography.

©2009 Optical Society of America

OCIS codes: (090.1995) Holography; Digital Holography, (110.6960) Tomography.

1. Introduction

Optical microscopy gives access to non-invasive and real-time imaging capabilities. However, classical methods do not provide quantitative analysis tools. Among other methods providing quantitative measurements, digital holographic microscopy (DHM) enables the access to both amplitude and phase of a wave which has interacted with an object, through interferometric measurement [1]. The access to the phase provides a quantitative indicator, which is interpreted differently depending on the experimental conditions. In transmission, the phase is the integrated phase shift induced by the sample; in reflection, the phase signal measures the object topography, in case of a highly reflective sample.

Since DHM is identical to classical microscopy in the sense of the imaging method, it implies that no depth information is recorded, i.e. that out-of-focus information is not removed from the reconstructed signal. In order to retrieve the three-dimensional information, a scan has to be introduced during the measurement procedure. Different scanning procedures can be applied, either by scanning the wavelength or the angle of the excitation light [2, 3]. The depth information recovered through this procedure can then be coupled to the quantitative phase measurements to get finally quantitative three-dimensional measurements.

2. Tomography Principle

As stated in the previous section, three-dimensional imaging applied to DHM requires a modification of the propagation vector k of the excitation light. This is due to the fact that collected spatial frequencies are situated on subdivision of a sphere [3], commonly called the Ewald sphere, which corresponds to the coherent transfer function (CTF) of DHM. Scanning gives access to surfaces situated on different spheres, making possible to reconstruct a three-dimensional transfer function. This implies that the k -vector has to be scanned either in direction – which corresponds to a change in angle – or in norm – which corresponds to a change in wavelength.

In the case of a change in propagation direction, different methods were used to perform this operation: one can make rotate the sample, in order to take the necessary views at different angles [4, 5], while it is also possible to scan the beam angularly [6, 7, 8]. While the purpose of each procedure is the same, i.e. acquiring data along the surface of the Ewald sphere, it was shown recently that the two approaches lead to different transfer functions, and therefore different resolutions along each axis [9].

When using a change in wavelength, the spatial frequencies of the different acquisitions are situated on spheres of different radius. The reconstruction in this case leads to optical slicing. This method found successful applications in reflection [10, 11, 12]. It was recently shown that an analog reconstruction can be obtained through another method, consisting in changing the propagation direction, so that the k_z component, parallel to the optical axis, is changed [13].

3. Results

As seen in the previous section, the two scanning methods used for tomographic measurements can be understood from the same theoretical framework. However, the data treatment itself is quite different, due to the nature of scanning employed. We present in this section tomographic measurements taken with the two approaches described above.

3.1 Multiple wavelength

Concerning the wavelength-scanned method, neither the object nor any part of the setup is mechanically moved. Different equally k -spaced wavelength full-field holograms are sequentially acquired, and the corresponding complex wavefronts are summed in order to add constructively in a plane of interest where they are in phase, and destructively in out-of-plane sections, resulting in a slicing effect. We developed a new approach enabling to detect for the first time the

reflection phase signal of fixed red blood cells (RBC), for which the membrane geometry in 3D can be retrieved thanks to the sub-micrometer resolution of the experimental configuration. Our tomography method is a refined version of the one employed in [11]: we apply a Kaiser weighting function to reduce the ripples of the axial filter function down to -15 dB, while the axial resolution reaches $1 \mu\text{m}$.

The sample is sequentially illuminated by 20 equally k-spaced wavelengths within the 485-670 nm range, generated with a tunable femtosecond optical parametric amplifier (OPA), with a coherence length (L_c) of about 60-75 μm . The optical configuration is a Mach-Zehnder interferometric reflection DHM setup with a 1.25 NA 100x oil immersion microscope objective. Once the hologram sequence is recorded, each complex wavefront is digitally reconstructed, and their phase offsets are equalized in a constant-phase reference plane $z = 0$ to avoid random addition. Finally, a phase-only wavefront addition is performed for a plurality of phase offset values to scan the sample in depth.

The results exposed below are obtained with red blood cells, namely a 90% Ethanol-fixed $4 \mu\text{l}$ blood solution suspended in a HEPA buffer (HEpes Potassium Albumin buffer) sandwiched by two 0.17 mm glass coverslips. The glass-sample interface of the upper coverslip is custom-designed with an anti-reflection coating reducing glass-water reflectivity down to 0.05%. Combined with an inverted geometry, this ensures that the extremely weak signal reflected by the RBC membrane is not lost among the intense glass-water reflection generated at the coverslip interface. By this way, direct on-cell phase reflection measure is now rendered possible.

Fig. 1.(a) shows thereafter for the first time cellular membrane reflection DHM phase images of a RBC. Then Fig.1.(b,c) compares the classical unitary and our Kaiser-weighted X-Z tomographic cut results on a $7.5 \mu\text{m}$ axial scale. Fig. 1.(e,f) finally show 3D point clouds corresponding to the whole 3D volume resulting from gathering all Kaiser X-Z cuts like Fig. 1.(c). From the results of Fig. 1, one can clearly identify the surrounding coverslip surface and the well-known biconcave shape of the RBC external membrane, despite the size of such cells being 2-3 μm high.

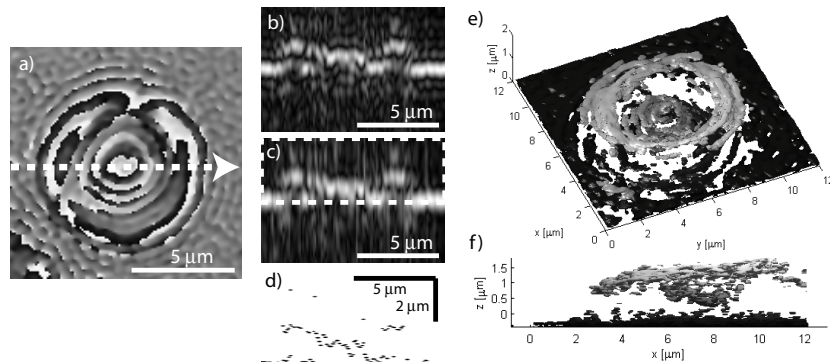


Figure 1: Tomography of a RBC. (a) Reflection DHM phase image; (b) Tomographic X-Z cut through the cell along as indicated by the white arrow in (a) with no weighting function; (c) Same as (b) but with Kaiser weighting function; (d) Peak-detected result applied on a zoomed region (white dashed rectangle) of (c); (e) 3D-representation of the series of peak-detected tomographic cuts as in (d) on the RBC of (a); (f) lateral view of (e).

3.2 Multiple angles

In the case of angle scanning, the optical setup is maintained static during measurement, while the sample is rotated perpendicularly to the optical axis. The rotation is achieved by clamping the observed object with a micropipette fixed on a motorised stage, so that it could be rotated within a chamber containing the immersion medium. The sample in this case is a tek amoeba [14], but our technique proved successful on other specimens, such as pollen grains [5]. The dataset is acquired with a rotation angle of 180° , and an angle sampling of 1° .

The sample is illuminated with a laser diode ($\lambda = 635 \text{ nm}$), and imaged with a $20\times 0.4 \text{ NA}$ microscope objective. The optical configuration corresponds to a Mach-Zehnder transmission DHM setup. The holograms being taken in the Fresnel region, each hologram is reconstructed and digitally focused in the Fresnel approximation [1]. A reference in phase has to be taken for each image outside the sample, in order to correct for eventual vibrations during scanning.

The phase has then to be unwrapped, because thick samples can induce phase shifts larger than a wavelength. Glycerol ($n = 1.473$) was selected in this case as the immersion medium, in order to minimise the amount of phase jumps present in the phase images, and decrease accordingly the amount of phase ambiguities, in order to ensure accurate unwrapping. From the unwrapped phase images, it is then possible to reconstruct the three-dimensional data with an inverse Radon transform. Since the refractive index of the medium is precisely known, it is possible to calibrate the setup directly from the measurements, and get the three-dimensional refractive index map of the biological sample.

Fig. 2.(a) presents a 3D visualization of a tek amoeba, where the internal structure can be readily identified. Each color, displayed with some transparency, represents a range of refractive index, showing clearly the amoeba with its internal structure (in yellow) within its shell (in blue). Fig. 2.(b) is a projection on the x-y plane, giving a better insight of the amoeba structure. Some internal elements in the amoeba are a few micron in size, showing that the tomographic reconstruction is close to the optical resolution of the setup.

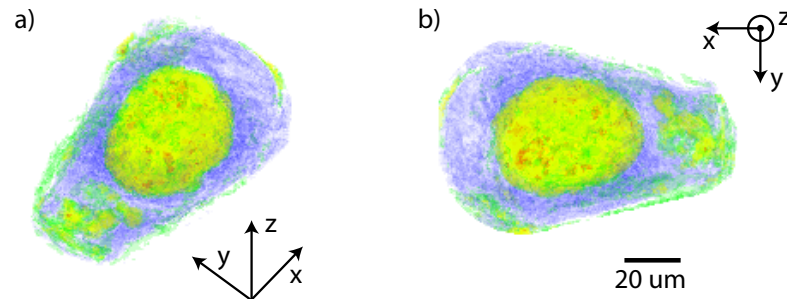


Figure 2: Transparency view of a tomographic measurement of a tek amoeba, in (a) angular view and (b) x-y projection. Colors correspond to refractive index value range: Blue: 1.448-1.467, Green: 1.474-1.478, Yellow: 1.478-1.493, Red: 1.493-1.513. The gap non represented corresponds to the refractive index of the immersion medium.

4. Conclusion

We presented results of tomographic measurements made with digital holographic microscopy, taken with two different methods, each using a different way of recovering the 3D information. One is based on wavelength scanning in reflection, leading to on-cell reflection measurements. The second is based on angular scanning in transmission, leading to 3D refractive index map of biological samples.

5. Acknowledgments

The authors would like to thank the members of the Microvision and Microdiagnostics group, and especially E. Shaffer, for the fruitful collaboration. This work was supported by the Swiss National Science Foundation (SNSF) grant # 205320-120118.

6. References

- [1] E. Cucho, P. Marquet, and C. Depeursinge, "Simultaneous amplitude-contrast and quantitative phase-contrast microscopy by numerical reconstruction of Fresnel off-axis holograms," *Appl. Opt.* **38**, 6994–7001 (1999).
- [2] E. Wolf, "Three-dimensional structure determination of semi-transparent objects from holographic data," *Opt. Commun.* **1**, 153–156 (1969).
- [3] R. Dändliker and K. Weiss, "Reconstruction of the three-dimensional refractive index from scattered waves," *Opt. Commun.* **1**, 323–328 (1970).
- [4] A. Barty, K. Nugent, A. Roberts, and D. Paganin, "Quantitative phase tomography," *Opt. Commun.* **175**, 329–336 (2000).
- [5] F. Charrière, A. Marian, F. Montfort, J. Kühn, T. Colomb, E. Cucho, P. Marquet, and C. Depeursinge, "Cell refractive index tomography by digital holographic microscopy," *Opt. Lett.* **31**, 178–180 (2006).
- [6] T. Noda, S. Kawata, and S. Minami, "Three-dimensional phase-contrast imaging by a computed-tomography microscope," *Appl. Opt.* **31**, 670–674 (1992).
- [7] M. Debailleul, B. Simon, V. Georges, O. Haeberlé, and V. Lauer, "Holographic microscopy and diffractive microtomography of transparent samples," *Meas. Sci. Technol.* **19**, 074009 (2008).
- [8] Y. Sung, W. Choi, C. Fang-Yen, K. Badizadegan, R. Dasari, and M. Feld, "Optical diffraction tomography for high resolution live cell imaging," *Opt. Express* **17**, 266–277 (2009).
- [9] S. Kou and C. Sheppard, "Image formation in holographic tomography," *Opt. Lett.* **33**, 2362–2364 (2008).
- [10] M. Kim, "Tomographic three-dimensional imaging of a biological specimen using wavelength-scanning digital interference holography," *Opt. Express* **7**, 305–310 (2000).
- [11] F. Montfort, T. Colomb, F. Charrière, J. Kühn, P. Marquet, E. Cucho, S. Herminjard, and C. Depeursinge, "Submicrometer optical tomography by multiple-wavelength digital holographic microscopy," *Appl. Opt.* **45**, 8209–8217 (2006).
- [12] M. Potoava and M. Kim, "Optical tomography for biomedical applications by digital interference holography," *Meas. Sci. Technol.* **19**, 074010 (2008).
- [13] S. Jeong and C. Hong, "Illumination-angle-scanning digital interference holography for optical section imaging," *Opt. Lett.* **33**, 2392–2394 (2008).
- [14] F. Charrière, N. Pavillon, T. Colomb, C. Depeursinge, T. Heger, E. Mitchell, P. Marquet, and B. Rappaz, "Living specimen tomography by digital holographic microscopy: Morphometry of testate amoeba," *Opt. Express* **14**, 7005–7013 (2006).